

Segmentation of Optic Disc in Retina Images using Texture

Suraya Mohammad¹, D. T. Morris¹ and Neil Thacker²

¹*School of Computer Science, University of Manchester, Kilburn Building, Oxford Road, Manchester, U.K.*

²*ISBE, Medical School, University of Manchester, Stop ford Building, Oxford Road, Manchester, U.K.*

Keywords: Optic Disc Segmentation, BRIEF, Texture.

Abstract: The paper describes our work on the segmentation of the optic disc in retinal images. Our approach comprises of two main steps; a pixel classification method to identify pixels that may belong to the optic disc boundary and a circular template matching method to estimate the circular approximation of the optic disc boundary. The features used are based on texture, calculated using the intensity differences of local image patches. This was adapted from Binary Robust Independent Elementary Features (BRIEF). BRIEF is inherently invariant to image illumination and has a lower degree of computational complexity compared to other existing texture measurement methods. Fuzzy C-Means (FCM) and Naive Bayes are the clustering and classifier used to cluster/classify the image pixels. The method was tested on a set of 196 images composed of 110 healthy retina images and 86 glaucomatous images. The average mean overlap ratio between the true optic disc region and segmented region is 0.81 for both FCM and Naive Bayes. Comparison with a method based on the Hough Transform is also provided.

1 INTRODUCTION

The evaluation of retinal images is a diagnostic tool widely used to gather important clinical information, such as for diabetic retinopathy and glaucoma assessment, due to its noninvasive nature. These diseases are two of the main cause of visual impairment worldwide (Congdon et al., 2003). Both are asymptomatic in nature, therefore early detection is vital to prevent complete visual loss. Segmentation of the optic disc represents the starting point of many automatic computer based methods used to assist the ophthalmologist in detecting these two diseases.

The Cup-to-Disc (CDR) ratio is commonly used clinically to assess glaucoma progression. CDR is obtained by measuring the ratio between the vertical diameter of the optic disc cup and the optic disc rim. As for diabetic retinopathy assessment, the identification of the optic disc is important to reduce misclassification in the automatic detection of other lesions.

Some of the difficulties experienced in the segmentation of the optic disc may be appreciated by Figure 1 which shows an image of a healthy retina (Figure 1(a)) and a glaucomatous retina (Figure 1(b)). On a healthy retina, the optic disc appears as bright and yellowish, normally with a circular or slightly elliptical shape. However these features and its size may vary between images. The contrast around the optic disc boundary is also not constant, normally brighter

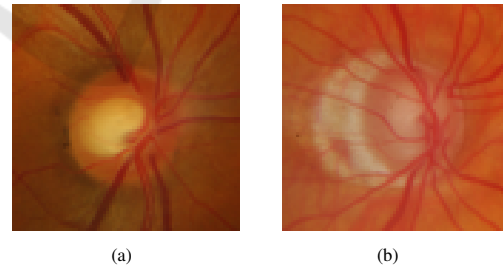


Figure 1: Healthy and glaucomatous retina images.

on the temporal side and less so on the nasal side. In addition, part of the optic disc boundary may be obscured by the outgoing blood vessels. Sometimes there exist bright regions near the edge of the disc caused by peripapillary atrophy (Figure 1(b)). This is more common in glaucomatous images compared to normal images. Retinal images also suffer from non uniform illumination due to how the image is captured. This non-uniform illumination results in shading artefacts and vignetting (Hoover and Goldbaum, 2003), hindering both quantitative image analysis and the reliable operation of subsequent global operators (Winder et al., 2009).

In this paper we present an automated segmentation of the optic disc combining pixel classification and circular template matching. We used texture features based on Binary Robust Independent Elementary Feature (BRIEF) (Calonder et al., 2010) to clas-

sify the image pixels. BRIEF is inherently invariant to image illumination, which in our opinion will handle the illumination issue faced by the retinal images. It also has a lower degree of computational complexity compared to other texture measurements. Naive Bayes and Fuzzy C Means (FCM) are used as the classifier and the clustering method respectively to classify/cluster the image pixels. To obtain the final circular approximation of the optic disc circular template matching is used. This is to approximate the optic disc boundary in the case of (1) not all of the optic disc boundary is detected and (2) there exist large gaps due to vessel passing in and out of the eye.

We validate our result with a retina image data set consisting of both normal and glaucomatous images. We also compare our result with another commonly known template matching approach, the Hough Transform.

2 LITERATURE REVIEW

A number of studies have reported work on optic disc segmentation. Among the existing techniques, the deformable or active contour (snake) has been used in (Joshi et al., 2011; Lowell et al., 2004; Morris and Donnison, 1999; Muramatsu et al., 2011). The main advantage of using this approach is the ability to obtain an accurate optic disc boundary. This is possible because the active contour has the ability to change shape depending on the properties of the image, desired contour properties and/or knowledge based constraints (Kass et al., 1988). There are two types of active contour currently used for optic disc segmentation, region based active contour or gradient-based active contour.

The gradient based active contour normally relies on the image gradient or edges to influence the energy forces to evolve to the true optic disc boundary. The presence of the blood vessels, atrophy, low contrast optic disc boundary and strong optic cup boundary may prevent the snake from evolving to the true optic disc boundary. Thus several preprocessing steps are often implemented prior to snake implementation, such as by performing blood vessel removal through morphological filtering as in (May, 2008) or histogram equalisation followed by thresholding and pyramid edge detection to enhance the edge (Morris and Donnison, 1999).

Region based active contour models on the other hand make use of statistical information from the background and foreground regions to minimise the energy function to best separate the regions (Joshi et al., 2011). The region based active contour is more

robust against local gradient variations. However in the case where the object to be segmented and the background regions are heterogeneous and have similar statistical model, erroneous segmentation may occur. Thus additional information such as local information from multiple image channels is used in (Joshi et al., 2011).

Another technique used for optic disc segmentation is circular and elliptical template matching. The Hough Transform is one of the commonest circular and elliptical template matching techniques used for optic disc segmentation. The matching is performed on an edge map extracted from the underlying image. The optic disc boundary found through this method is an approximation and may be not as precise as that obtained from deformable contour. One main advantage of the Hough Transform technique is that it is relatively unaffected by noise and gaps in the edge feature (Lowell et al., 2004). Thus it is very useful when attempting to determine the optic disc contour which has no clearly defined edges and is broken by ingoing and outgoing blood vessels. However obtaining good edge descriptors is vital for the success of the Hough transform. Otherwise unacceptable results may be given such as hitting either the curved blood vessel segments or the strong cup boundary (Lowell et al., 2004).

Recently pixel classification has been used to segment the optic disc. Pixel classification is where every pixel in the retina image will be classified into a class, such as optic disc or background. In (Muramatsu et al., 2011), Fuzzy C Means (FCM) and Artificial Neural Networks (ANN) are used to cluster and classify image pixels as optic disc or background pixels. For FCM Clustering, two pixel features were used, the median pixel value in the red channel and the mean pixel's values in the blood vessel erased image. Both are calculated over the surrounding 15x15 pixels. As for ANN three different pixel features were used. They are the pixel value in the red channel of the original image, and the blood vessel erased image and the presence of edges in the surrounding 3x3 pixels. They compared the result of the pixels classification with the result obtained by the snake method and show that pixel classification is able to demonstrate comparable performance to the snake approach.

Retinal images are acquired with a digital fundus camera, which captures the illumination reflected from the retinal surface. Due to the small size of the objects and the complexities of the optic system involved during the imaging process, retinal images are often affected by non uniform illumination. Figure 2 shows an example of a retina image with uneven illumination. The retina images affected by this are

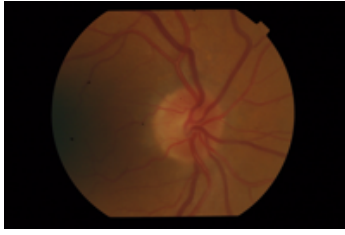


Figure 2: Samples of a retina image suffers from non uniform illumination.

normally brighter in the central region and darker in the periphery. The exact properties of illumination change may vary from image to image. Uneven illumination may alter the local statistical characteristics of the image intensity such as the mean and median and thus limits the reliable operation of any global image processing (Winder et al., 2009).

The existence of a large number of works on retina image illumination correction emphasize the importance of correcting the image illumination prior to further processing. This is normally done by preprocessing the images. The main aim of this preprocessing is to obtain images with a common standardised value to be used for subsequent processing or analysis. Some of the preprocessing methods used to correct the uneven illumination are briefly described next.

Illumination equalisation technique is used (Hoover and Goldbaum, 2003) for illumination correction. In this method each pixel is adjusted based on the desired intensity and its local average intensity. Work by (Cree et al., 1999) and (Foracchia et al., 2004) use a method based on the image formation model to correct the illumination. This method is based on the principle of the image formation model which states that a captured image is made up of two independent functions: the underlying image and the degradation model. Thus to correct the image, a degradation model of the image is estimated and then used to restore the underlying image.

Shade correction is another technique used to correct the non uniform illumination. It is based on the same principle as the image formation model above. The background image is approximated either (1) by smoothing the original image with mean/median filter as in (Spencer et al., 1996) or (2) using alternating sequential filters as in (Walter and Klein, 2002). Then the filtered image is subtracted from the original image to recover a more uniformly illuminated image.

The above approaches estimate the correction from the whole image, thus the result can be a generalised smoothing (Foracchia et al., 2005). To rectify this later techniques have used specific retinal features to contribute to the overall image correction. Vessel

pixels are proposed in (Wang et al., 2001) and background pixels are used in (Foracchia et al., 2005; Joshi and Sivaswamy, 2008; Grisan et al., 2006) to estimate the illumination correction. Once the estimate is obtained, it will be used to normalise the original image.

Although the preprocessing steps have been shown to improve performance in some automatic detection system (Youssif et al., 2007), but in some other experiment they are not (Ricci and Perfetti, 2007). Retinal images consist of many features e.g., optic disc and various types of lesions, and these features can be very important especially as diagnostic evidence for many diseases. Thus care must be taken while performing this preprocessing step, so that the these features are preserved. Small structures such as the thinnest blood vessel may become lost and image noise may be amplified (Ricci and Perfetti, 2007).

Our work contributes to the use of pixel classification for optic disc segmentation. Instead of using pixel features based on statistical pixel features such as mean and median, we used texture. We have chosen to characterise texture using BRIEF which is already invariant to image illumination. Since the retina image suffers from non-uniform illumination we believe this texture measurement is worth doing. And in doing so, we avoid doing the preprocessing explained above.

3 METHODS

The objective of this work is to implement optic disc segmentation. The proposed method combines pixel classification using texture and circular template matching. The procedure is illustrated in Figure 3 and consists of 3 main steps:

1. **Feature Extraction.** Regions surrounding each pixel from each colour (red, green and blue) channel are transformed into their BRIEF representation or descriptor. In addition to all the three channels, to ensure that we utilise the available colour information in the retina image, we also combine the BRIEF descriptor from those separate channels into an RGB descriptor. To form the RGB descriptor, the descriptors are concatenated into a single binary string. For example assuming a 16 bits descriptor is used to represent a pixel in each colour channel, then the resulting descriptor for that pixel in the RGB channel is 48 bits long. These representations are then used for classification.
2. **Classification:** Naive Bayes and Fuzzy C Means (FCM) are the selected classifier and clustering

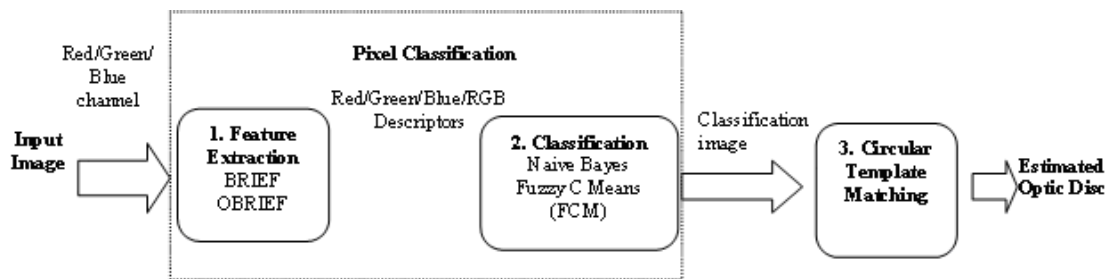


Figure 3: Flow Chart of the methods

methods used to classify/cluster each pixel into one of two classes, 'optic disc' and 'background'.

- 3. Circular Template Matching.** This last stage is to obtain the final circular approximation of the optic disc. This will handle the gaps caused by ingoing and outgoing blood vessels near the optic disc boundary and will approximate the optic disc boundary if not all of the boundary is detected.

3.1 Binary Robust Independent Elementary Feature (BRIEF)

BRIEF (Calonder et al., 2010) uses binary vectors to represent image patches. It takes a smoothed image patch and computes the result of the binary test between sets of pairs of pixel intensities. The location of the pixels pairs are predefined either randomly or in systematic pattern and lies within the patch. The feature descriptor for a patch is then defined as a vector of n binary tests.

Two important considerations when computing BRIEF descriptors are the smoothing kernel to be used and the spatial arrangement of the pixel pairs. Smoothing is introduced to suppress noise, thus increasing the stability and repeatability of the descriptors (Calonder et al., 2012). However smoothing may cause loss of spatial image detail, because of that we adopted the method used in (Tar and Thacker, 2011), i.e. we estimate the noise level beforehand and use it as a threshold when calculating the BRIEF descriptors. In this works, the test locations (the pixel pairs) are defined randomly within the patch.

The formal definition of the BRIEF descriptor used in our work is as follows:

A test τ defined on patch p of size $S \times S$ as

$$\tau(p; \underline{x}, \underline{y}) = \begin{cases} 1 & \text{if } (p(\underline{x}) - p(\underline{y})) > \text{Threshold} \\ 0 & \text{otherwise} \end{cases} \quad (1)$$

where $p(\underline{x})$ and $p(\underline{y})$ are the pixel intensities at locations \underline{x} and \underline{y} .

The BRIEF descriptor is defined as the n bit vector

$$f_n = \sum_{1 \leq i \leq n} 2^{i-1} \tau(p; \underline{x}_i, \underline{y}_i) \quad (2)$$

We choose $S = 27$ and $n = 16$. Other combinations of S and n were considered and tested with a smaller number of training cases. The above mentioned parameters were selected as they gave the best result. The threshold is set to 3 times the estimated image's noise magnitude.

3.2 Naive Bayes Classifier

Naive bayes (Duda et al., 2001) is used as a sample of supervised learning. It has the advantages of simplicity, computational efficiency, and good classification performance and in some cases is able to outperform more sophisticated classifiers.

Since the BRIEF features are binary, given a finite set of features then Bayes theorem can be expressed as:

$$P(\omega_i|x) = \frac{P(x|\omega_i)P(\omega_i)}{P(x)} \quad (3)$$

Where ω_i is the i^{th} class. $P(\omega_i)$ is a priori probability of class ω_i , $P(x|\omega_i)$ is the likelihood of feature vector x given a class ω_i and $P(\omega_i|x)$ is the posterior probability of class ω_i given observation x , i.e. the result of the Bayes rule. $P(x)$ is the normalisation constant. We estimate $P(\omega_i)$ and $P(x|\omega_i)$ from the training data. The decision rule used for classification is based on maximum a posterior (MAP), i.e. choose the class with the highest $P(\omega_i|x)$.

We used Naives Bayes with two fold cross validation. BRIEF features from the optic disc and background are used to train the Naive Bayes.

3.3 Fuzzy C Means (FCM)

FCM clustering is selected as a sample of unsupervised learning. One of the advantages of unsupervised

learning is that it is not dependent on the training data, and thus it is generalisable to new cases. FCM is a method of clustering where each point may belong to one or more clusters with different degree of membership (Bezdek, 1981). The features with close similarity in an image are grouped into the same clusters. Similarity is defined as the distance from feature vectors to the cluster's centre.

FCM is based on minimisation of the objective function in equation 4, by iteratively updating the membership u_{ik} and cluster centre v_i :

$$J = \sum_{k=1}^N \sum_{i=1}^C u_{ik}^m \|x_k - v_i\|^2 \quad (4)$$

where N is the number of data points, C is the number of clusters, x_k is the k th data point, v_i is the i th cluster centre, u_{ik} is the degree of membership of k th in the i th cluster and m is a constant greater than 1 (normally 2), used to determine the fuzziness of the clusters. In this study the number of cluster is chosen as two, optic disc and background cluster.

The membership degree, u_{ik} and the cluster centre v_i are defined by:

$$u_{ik} = \frac{1}{\sum_{j=1}^C \left(\frac{\|x_k - v_i\|}{\|x_k - v_j\|} \right)^{\frac{2}{m-1}}} \quad (5)$$

$$v_i = \frac{\sum_{k=1}^N u_{ik}^m x_k}{\sum_{k=1}^N u_{ik}^m} \quad (6)$$

Given the desired number of clusters and initial value of cluster centres, the FCM will converge to a solution for v_i that represents a local minimum or saddle point of the cost function J (Bezdek, 1981).

3.4 Circular Template Matching

To approximate the circular boundary of the optic disc we use circular and elliptical template matching. The templates are of various diameters and orientations (see examples in Figure 4), and these templates will be cross correlated with the classification result images. The matching process is done in parallel in the four classification images from the red, green, blue and RGB channel.

The correlation coefficient was used to present an indication of the match between the template image and the classification image. The final decision of the good match is taken as the one with the highest correlation value.



Figure 4: Samples of the template used.

4 TESTING AND RESULT

The image database used in this study is made up of 196 images. 110 images are normal and 86 are glaucomatous images. These images were kindly provided by Manchester Royal Eye Hospital.

The algorithm performance was evaluated by measuring the overlap area, using an overlapping score (O) between the ground truth optic disc region and the approximated regions obtained from the described approach, defined as below:

$$O = \frac{Area(G \cap S)}{Area(G \cup S)} \quad (7)$$

where O is the overlap area, G is the ground truth region and S is the segmented region by the proposed approach. An overlap area of '1' indicates perfect agreement between ground truth and the proposed approach. For the determination of CDR value, the vertical length of the disc region is often measured. Therefore average errors in the largest vertical length of the disc region are also calculated.

The results are shown in Table 1 and Table 2. The average overlap area between the ground truth and the segmentation result by FCM and Naive Bayes are 0.85 and 0.84 for the normal set respectively. For the glaucomatous set of images the overlapping score for FCM and Naive Bayes is 0.77. In the classification image result using FCM, the optic disc boundary is more pronounced thus giving a slightly better performance.

As expected the average overlapping area result in the glaucomatous set is slightly lower than the normal set. The reason is that glaucoma deforms the optic disc shape making it less conforming to the standard shape of our templates. In addition, a larger number of images in this set show signs of atrophy. Atrophy shares similar characteristic to the optic disc, thus atrophy regions are misclassified as optic disc pixels. In the case of severe atrophy the image is either over segmented or under segmented. Samples of segmented optic discs are shown in Figure 5.

A good segmentation result is obtained in an image with a good contrast and clear optic disc boundary. The system also managed to get good approximation in an image with incomplete optic disc boundary and the presence of mild atrophy. Poor segmentation

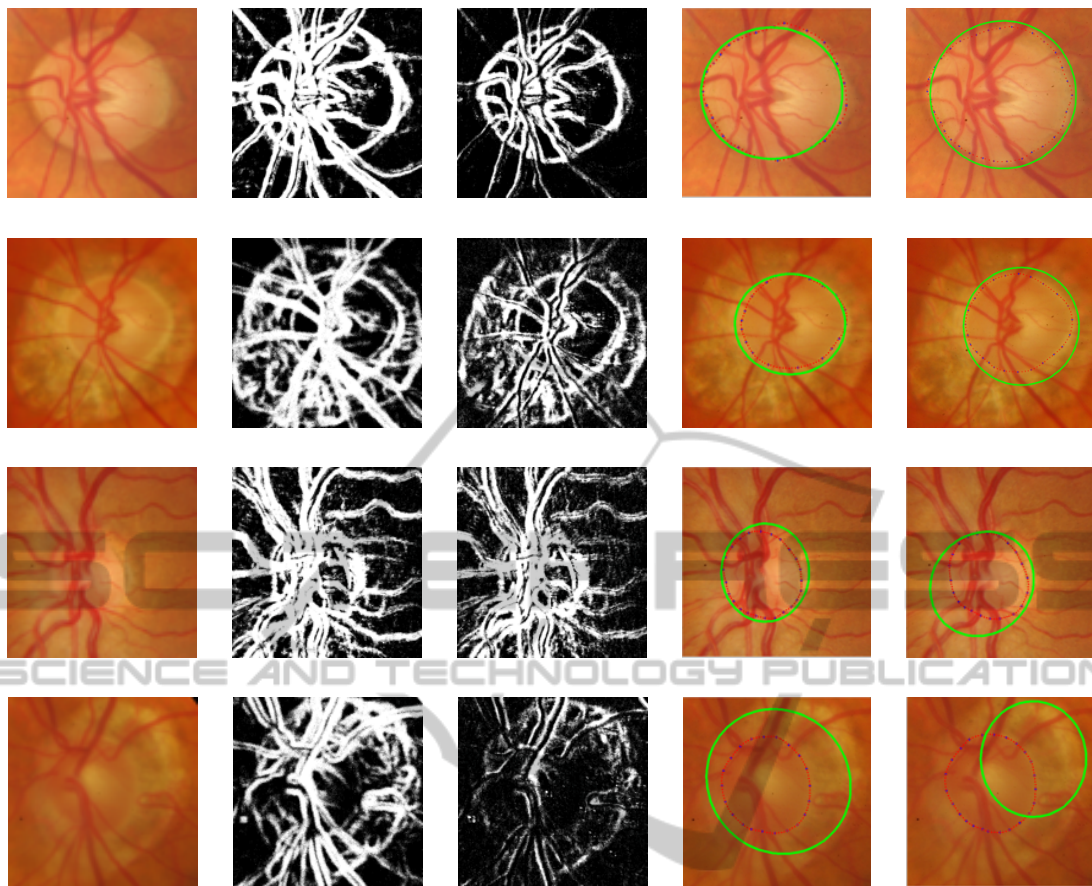


Figure 5: This figure illustrates the process of segmenting the optic disc, performed on the colour combination channel. The first and fourth rows are images from the normal images set. The second and third row are images from the glaucomatous set. From left to right: Original image, classification image using FCM, classification image using Naive Bayes, optic disc boundary approximation using FCM and optic disc boundary approximation using Naive Bayes. The dotted line is the ground truth and the green line is the approximated boundary.

Table 1: Disc segmentation result by the Fuzzy C Means.

	Average overlapping ratio	Vertical length error (%)	Horizontal length error (%)
Normal	0.85	3.1	4.3
Glaucoma	0.77	5.8	6.0
All	0.81	4.5	5.2

Table 2: Disc segmentation result by the Naive Bayes.

	Average overlapping ratio	Vertical Length error (%)	Horizontal Length Error (%)
Normal	0.84	4.9	5.2
Glaucoma	0.77	7.1	8.6
All	0.81	6	6.9

results are normally obtained from an image with either severe atrophy (Figure 5:row 4), or with quite a number of thick vessels passing in and out of the optic disc (Figure 5:row 3) and those with irregular shape.

We also compared our result to another common

template matching approach that is the Hough transform as implemented in (May, 2008). The Hough Transform is performed based on the edges obtained by the Canny edge detector. Vessel removal is implemented prior to the edge detector. The evaluation used in their work is based on calculating the discrepancy (D) between two closed boundary curves or contour described as:

$$D(G_c, S_c) = \frac{\frac{1}{2} \left\{ \frac{1}{n} \sum_{i=1}^n d(g_{ci}, S) + \frac{1}{m} \sum_{i=1}^m d(s_{ci}, G) \right\}}{G_d} \quad (8)$$

G_c and S_c are the contours of the segmented area in the ground truth and segmented images. $d(a_i, B)$ is the minimum distance from point i on the contour A to any point on the contour B . G_d is the diameter of the ground truth contour. A low discrepancy value implies a better segmentation performance.

The comparison result is shown in Table 3. As can be seen, our approach shows improvement in minimising the discrepancy over the Hough Transform method. Figure 6 shows a sample image where the optic disc is successfully segmented by all three methods (Row 1) and an image where our approach shows a better segmentation result compared to the Hough Transform (Row 2). In this particular case, the Hough Transform is trapped by the strong optic cup boundary.

Table 3: Average Discrepancy (D) by the three methods.

	FCM	Naive Bayes	Hough Transform
Normal	0.06	0.06	0.10
Glaucoma	0.09	0.09	0.13
All	0.08	0.08	0.12

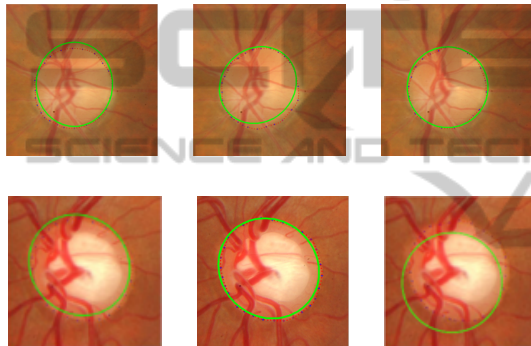


Figure 6: Comparisons of disc outlines determined by the three methods. From left to right: Optic disc boundary approximation based on clustering result by FCM clustering and optic disc boundary approximation based on classification result by Naive Bayes and optic disc approximation by the Hough Transform. The dotted line is the ground truth and the green line is the approximated boundary.

5 CONCLUSIONS AND FUTURE WORKS

A method for optic disc segmentation is presented in this paper. We demonstrate that the proposed method is at least as reliable as other algorithms for the optic disc segmentation with the advantages of computational simplicity. An interesting property of our method is the use of an illumination invariant texture measurement to address the illumination issue of the retina images. Furthermore, by making use of machine learning techniques in our approach, we can exploit the knowledge of the characteristics of the optic disc in the segmentation process.

Nonetheless, the method has several limitations which we aim to address in future research. We used training data to model the optic disc characteristic

with the hope of better discrimination between optic disc and background pixels (including vessels and atrophy pixels). However, some miss classification between pixels on the vessel boundaries, atrophy and optic disc boundary do occur in some of the images. Thus in future we intend to (1) implement a rotation invariant version of BRIEF as an attempt to reduce miss classification of vessels and (2) ensure that data used for training the Naive Bayes includes sufficient number of atrophy pixels so that the result may improve. At the moment the pixels used in the training data were randomly selected.

Another problem is the use of circular/elliptical template matching. Quite often, this approach fails to get good segmentation in cases where the optic disc is not of 'standard' shape. Therefore we are currently looking at ways to trace the boundary from the classification image guided by the obtained circumference given by the template matching approach.

REFERENCES

- Bezdek, J. C. (1981). *Pattern recognition with fuzzy objective function algorithms*. Kluwer Academic Publishers.
- Calonder, M., Lepetit, V., Ozuysal, M., Trzcinski, T., Strecha, C., and Fua, P. (2012). Brief: Computing a local binary descriptor very fast. *Pattern Analysis and Machine Intelligence, IEEE Transactions on*, 34(7):1281–1298.
- Calonder, M., Lepetit, V., Strecha, C., and Fua, P. (2010). Brief: binary robust independent elementary features. In *Computer Vision—ECCV 2010*, pages 778–792. Springer.
- Congdon, N. G., Friedman, D. S., and Lietman, T. (2003). Important causes of visual impairment in the world today. *JAMA: the journal of the American Medical Association*, 290(15):2057–2060.
- Cree, M. J., Olson, J. A., McHardy, K. C., Sharp, P. F., and Forrester, J. V. (1999). The preprocessing of retinal images for the detection of fluorescein leakage. *Physics in Medicine and Biology*, 44(1):293–308. Cited By (since 1996):18.
- Duda, R., Hart, P., and Stork, D. (2001). *Pattern classification*. Wiley, pub-WILEY:adr, second edition.
- Foracchia, M., Grisan, E., and Ruggeri, A. (2004). Detection of optic disc in retinal images by means of a geometrical model of vessel structure. *IEEE Transactions on Medical Imaging*, 23(10):1189–1195.
- Foracchia, M., Grisan, E., and Ruggeri, A. (2005). Luminosity and contrast normalization in retinal images. *Medical Image Analysis*, 9(3):179–190.
- Grisan, E., Giani, A., Ceseracciu, E., and Ruggeri, A. (2006). Model-based illumination correction in retinal images. In *Biomedical Imaging: Nano to Macro, 2006. 3rd IEEE International Symposium on*, pages 984–987. IEEE.

- Hoover, A. and Goldbaum, M. (2003). Locating the optic nerve in a retinal image using the fuzzy convergence of the blood vessels. *Medical Imaging, IEEE Transactions on*, 22(8):951–958.
- Joshi, G. D. and Sivaswamy, J. (2008). Colour retinal image enhancement based on domain knowledge. In *Computer Vision, Graphics & Image Processing, 2008. ICVGIP'08. Sixth Indian Conference on*, pages 591–598. IEEE.
- Joshi, G. D., Sivaswamy, J., and Krishnadas, S. (2011). Optic disk and cup segmentation from monocular color retinal images for glaucoma assessment. *Medical Imaging, IEEE Transactions on*, 30(6):1192–1205.
- Kass, M., Witkin, A., and Terzopoulos, D. (1988). Snakes: Active contour models. *International journal of computer vision*, 1(4):321–331.
- Lowell, J., Hunter, A., Steel, D., Basu, A., Ryder, R., Fletcher, E., and Kennedy, L. (2004). Optic nerve head segmentation. *Medical Imaging, IEEE Transactions on*, 23(2):256–264.
- May, M. (2008). Automatic Detection of the Optic Disc Within Retinal Images. Master's thesis, University of Manchester, UK.
- Morris, D. and Donnison, C. (1999). Identifying the neuroretinal rim boundary using dynamic contours. *Image and Vision Computing*, 17(3):169–174.
- Muramatsu, C., Nakagawa, T., Sawada, A., Hatanaka, Y., Hara, T., Yamamoto, T., and Fujita, H. (2011). Automated segmentation of optic disc region on retinal fundus photographs: Comparison of contour modeling and pixel classification methods. *Computer methods and programs in biomedicine*, 101(1):23–32.
- Ricci, E. and Perfetti, R. (2007). Retinal blood vessel segmentation using line operators and support vector classification. *Medical Imaging, IEEE Transactions on*, 26(10):1357–1365.
- Spencer, T., Olson, J., McHardy, K., Sharp, P., and Forrester, J. (1996). An image-processing strategy for the segmentation and quantification of microaneurysms in fluorescein angiograms of the ocular fundus. *Computers and Biomedical Research*, 29(4):284–302.
- Tar, P. and Thacker, N. (2011). A quantitative representation for segmentation of martian images. Technical report, ISBE, Medical School, University of Manchester.
- Walter, T. and Klein, J.-C. (2002). A computational approach to diagnosis of diabetic retinopathy. In *Proceedings of the 6th Conference on Systemics, Cybernetics and Informatics (SCI2002)*, pages 521–526.
- Wang, Y., Tan, W., and Lee, S. C. (2001). Illumination normalization of retinal images using sampling and interpolation. In *Medical Imaging 2001*, pages 500–507. International Society for Optics and Photonics.
- Winder, R., Morrow, P., McRitchie, I., Bailie, J., and Hart, P. (2009). Algorithms for digital image processing in diabetic retinopathy. *Computerized Medical Imaging and Graphics*, 33(8):608 – 622.
- Youssif, A. A., Ghalwash, A. Z., and Ghoneim, A. S. (2007). A comparative evaluation of preprocessing methods for automatic detection of retinal anatomy. In *Proceedings of the Fifth International Conference on Informatics and Systems (INFOS 07)*, pages 24–30.